Effect of Pore Fluid Pressure on Slip Behavior of Experimental Fault with Gouge

Dashaun Horshaw

4/25/2019

Advisor: Dr. Wenlu Zhu

GEOL 394

I. ABSTRACT

Injecting fluids into the crust is a way to dispose of wastewater during natural gas and oil exploration. The injection of fluids into the crust has led to regional increases in seismicity. The increase in seismicity can be explained by an increase in pore fluid pressure along preexisting faults which decreases the effective normal stress on the fault. The frictional resistance, being proportional to the effective normal stress, is also decreased. With less resistance, a lower shear stress is needed to accommodate slip along the fault. However, recent experiments do not account for a gouge layer along the fault, something that occurs frequently in natural rock. Fault gouge is a layer of crushed rock and contains voids that can hold the water. The gouge could not only affect the critical stress of the fault but also affect the behavior of the slip during failure. In order to properly characterize the effect of pore fluid pressure and in turn fluid injection, there needs to be an observation of faults with a gouge.

As part of this work, I investigated the effect of pore fluid pressure on an experimental fault with gouge, and in term, the effect on the critical stress and slip behavior, by an experimental triaxial load apparatus. The experimental fault was composed of Berea Sandstone with a quartz gouge. The sample was then loaded into the apparatus that is able to servo control the confining and pore fluid pressures acting on the sample. The apparatus increased the normal stress acting on the sample until it fails and slips. This was performed four different times at four different pore fluid pressures. The results of the pore fluid pressure increasing was observed and recorded.

The effect on the critical shear stress was evaluated by observing the different yield stress recorded during varying pressure conditions. A difference of 60 MPa in pore fluid pressure increased the yield stress by 15.39 MPa. The slip behavior was evaluated by recording the varying slip frequencies and stress drops during the slip, during varying pressure conditions. A difference of 60 MPa decreased the frequency of slip by 0.003 Hz and increased the stress drops by 4.8 MPa.

From this investigation and previous experiments, it was deduced that the increase of pore fluid pressure leads to an increase in yield stress, and therefore critical stress. This is due to the pore fluid pressure strengthening the sample before failure. An increase in fluid pore pressure resulted in a decrease in frequency of slip but an increase in stress drop. Although the strengthening lead to longer time between the slips, the high fluid pore pressure leads to more drastic differences in stress during the slip.

In real world relations, this can be applied to fluid injection and realizing the effect fluid injections will have on the surrounding area. A high pore fluid pressure will allow for a higher critical shear stress to be reached, while also providing a higher magnitude seismic activity. This work will aid in future geologic exploration that include wastewater injection by properly characterizing the effect of pore fluid pressure on the critical stress and slip behavior on a fault with gouge and allowing geologic scientist to take necessary precautions during fluid injection.

II. TABLE OF CONTENTS AND LIST OF FIGURES AND TABLES

Table of Contents

I. Abstract……...Page 2
II. Table of Contents……Page 3
III. Introduction……Page 5
IV. Background Information……Page 6
V. Hypothesis……...Page 8
VI. Method of Analysis……Page 8
VII. Presentation of Data and Analysis of Uncertainty……Page 11
VIII. Discussion of Results……....Page 24
IX. Suggestions for Future Work……Page 26
X. Conclusions……...Page 26
XI. Acknowledgements……...Page 27
XII. Appendix……...Page 28
XIII. Bibliography…… Page 34

List of Figures

Figure 1. Mohr's Circle……...……Page 6

Figure 2. Earthquakes with Magnitude Above 3……...…….....Page 7

Figure 3. Diagram of Apparatus……...……...…….....Page 9

Figure 4. Picture of Apparatus……...…….....Page 9

Figure 5. Berea Sandstone Cylinder…….……...……. Page 10

Figure 6. Sandstone Wrapped in Foil…...……...……. Page 10

Figure 7. Completed Sample……...……. Page 11

Figure 8. Loading Jacket……...……... Page 11

Figure 9. Experiment 1 Pressure Variables.……...……. Page 12

Figure 10. Experiment 1 Shear Stress…….……...……. Page 13

Figure 11. Experiment 1 Expanded View.……...…….....Page 14

Figure 12. Experiment 2 Pressure Variables.……...……...…. Page 15

Figure 13. Experiment 2 Shear Stress…….……...……. .Page 16

Figure 14. Experiment 2 Expanded View……...…….Page 17

Figure 15. Experiment 3 Pressure Variables.……...…….Page 18

Figure 16. Experiment 3 Shear Stress…….……...……...…....Page 19

Figure 17. Experiment 3 Expanded View.……...…….Page 20

Figure 18. Experiment 4 Pressure Variables.……...…….Page 21

Figure 19. Experiment 4 Shear Stress…….……...……...Page 22

Figure 20. Experiment 4 Expanded View.……...…….Page 23

Figure 21. Sample After Deformation.……...……...……...Page 25

Figure 22. Experiment 2.2 Pressure Variables.……... Page 28

Figure 23. Experiment 2.2 Shear Stress…..……...……....Page 29

Figure 24. Experiment 2.2 Expanded View.……...……..Page 30

Figure 25. Experiment 2.3 Pressure Variables.……... Page 31

Figure 26. Experiment 2.3 Shear Stress…..……...……Page 32

Figure 27. Experiment 2.3 Expanded View.……...……..Page 33

List of Tables

Table 1. Trial Descriptions…….……...……. Page 8

Table 2. Ranges and Precisions…….……...…….Page 24

Table 3. Pressure Variables…….……...……...Page 24

Table 4. Frequency of Slips…….……...……. Page 25

Table 5. Average Stress Drop…….……...……...Page 25

Table 6. Yield Stress…….……...……. Page 26

III. INTRODUCTION

Earthquakes release stored elastic strain energy when a fault slips [Ellsworth, 2013]. Geologic engineering practices that include wastewater disposal can increase pore fluid pressure (referred to also as pore pressure) and reactivate faults, causing slip resulting in increased seismic hazards [Keranen *et al.*, 2013; French *et al*., 2016; Geobel and Brodsky, 2018]. Wastewater injection is correlated to regional increases in seismic activity [Ellsworth, 2013; Keranen *et al.*, 2013; Keranen *et al.*, 2014]; however, the earthquakes caused by fluid injection are usually not felt at the surface. Low magnitude earthquakes (< 3 on Richter scale) are rarely felt at the Earth's surface. Many of these earthquakes caused by fluid injection are low magnitude due to a lack of slip occurring or the slip being aseismic [Ellsworth, 2013]. While induced seismicity remains an issue, efforts to minimize the effects of wastewater injection can be made by understanding the fundamental processes and geologic factors that cause faults to slip seismically during fluid injection [French *et al*., 2016]. Geophysical observations led to indication of controls for slip such as fault orientation [Frohlich *et al.*, 2015]. However, the fluid injection changes the pore fluid pressure on the fault. There are efforts to create a slip model to better understand the effect of pore fluid pressure. However, constraining the controls of the occurrence and style of fault slip is difficult, due to regional differences in injection history, lithology, structure, and stress state [French *et al*., 2016].

The previously mentioned slip model also does not include the effect of fault gouge. Fault gouge is a layer of crushed and broken rock produced by friction between the two sides of rock moving along the fault. In natural faults, the fluid flow and mechanical properties of fault gouge materials are potential controls for pore fluid pressure and by relation, effective normal stress and critical shear stress.

In this experimental investigation, the effect of pore fluid pressure on a fault is examined with inclusion of a gouge layer. Slip under set confining pressures, to replicate a fault, and pore fluid pressures, to replicate the effect of fluid injection, in order to investigate the reactions these variables have on the slip behavior, with gouge. These results of varying confining pressures and pore fluid pressures are compared, and the comparison shows how these two will affect the fault slip behavior. With a better understanding of the relationship of these two variables, I look to better characterize the effect of pore fluid pressure on slip behavior.

IV. BACKGROUND INFORMATION

Faulting and Critical Stress

Fault slip can be replicated by a model whereby slip occurs when the shear stress along the fault, τ, reaches a critical value, τC. This can be shown with a Mohr's circle where the x-axis is normal stress and the y-axis is shear stress [Fig. 1]. The critical shear stress can be calculated by $\tau C = \mu(\sigma n - Pf) + \tau_0$ (τ_0 *usually = 0)*, where μ is the coefficient of sliding friction of the rock ($0.6 \leq \mu \leq 0.85$ for most rocks) [Byerlee, 1978], and Pf is pore fluid pressure. The normal stress is replaced by $\sigma n' = \sigma n - Pf$, the "effective normal stress" for a given normal stress on the fault, σn. The above equations show increasing the pore fluid pressure, by fluid injection or other natural sources, would cause a corresponding decrease in the effective normal stress. This would also decrease the critical shear stress, and according to the threshold model, slip occurs when the critical shear stress is reduced to the resolved shear stress along the fault [French *et al.,* 2016].

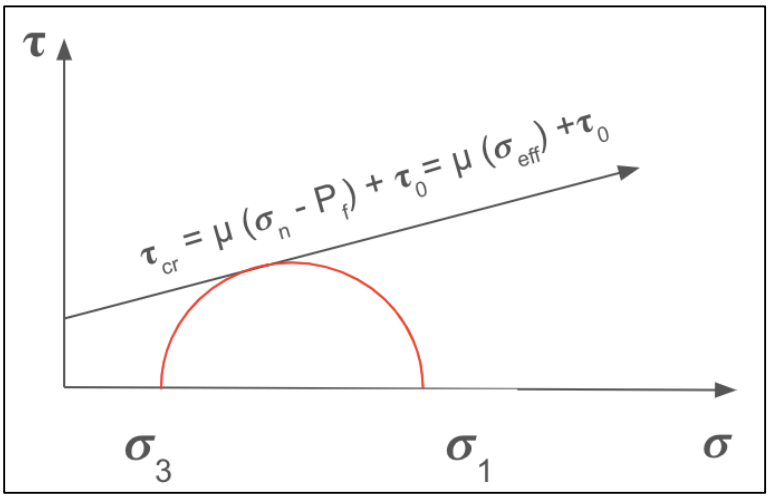

Fig 1: Mohr's Circle showing relationship between normal stress and shear stress. The equation for shear stress is shown. When the circle hits the line, the subject reaches failure.

The modeling of slip faults has been investigated and examined in many previous studies. A relationship between pore pressure and horizontal stress (σ_h) can be made by taking periodic pressure measurements during depletion of oil fields and virgin pressure measurements in sedimentary basins [Hillis, 2000]. Simple, uncoupled models do not include fault gouge. Differential stress, (σ_v - σ_h), in normal fault regime basins increases as pore pressure decreases and decreases as pore pressure increases. However, if the pore pressure is increased and the differential stress is decreased, it implies that a greater increase in pore pressure can be accommodated prior to failure than would otherwise be predicted. There is an increase in the propensity of faulting material tensile strength, rather than shear failure threshold. Depletion-induced seismicity can be explained by increased differential stress with decreased pore pressure and increased effective stress.

Given that it is believed that increasing fluid pressure along preexisting faults will increase seismicity rates due to the lower of the critical shear stress, τ_c, but the observed processes of slip under fluid pressurization are poorly constrained. Through experimental rock deformation with controlled fluid pressurization and pressurization rates on fault slip style, pore fluid pressurization was shown to be less effective than mechanical changes in fault normal stress at initiating accelerated slip events in faults [French *et al.*, 2016]. Fluid pressurization enhances the total slip distance, slip velocity, and shear stress drop (difference in maximum and

minimum values of slip) of events initiated by mechanical changes in normal stress. These parameters are directly correlated with pressurization rate. Magnitude of fluid pressure is not correlated.

Increase in Seismicity

Oil and natural gas exploration have been on the rise over the past couple of decades. Subsequently there has been an increase in seismic activity in areas that have frequent exploration activity [Fig. 2]. While majority of wastewater disposal wells operate aseismically, there is evidence many wells were capable of inducing earthquakes with magnitudes of up to 5 on the Richter scale [Ellsworth, 2013; Keranen *et al.,* 2013; Keranen *et al.,* 2014; Kim, 2013]. Oklahoma is one area in the central United States that has seen frequent seismic activity interpreted to be due to wastewater well injection. Initial fault rupture planes have also been observed relatively close to wastewater wells furthering the support of the wells are responsible for the induced earthquakes [Keranen *et al.,* 2013; Keranen *et al.,* 2014; Kim, 2013]. The water in the wastewater wells causes an increase in pore fluid volume lowering effective stress [Keranen *et al.,* 2013]. The fault activity close to the injection indicates that the expanding high fluid pressure front increased the pore pressure along its path and progressively triggered the earthquakes [Kim 2013].

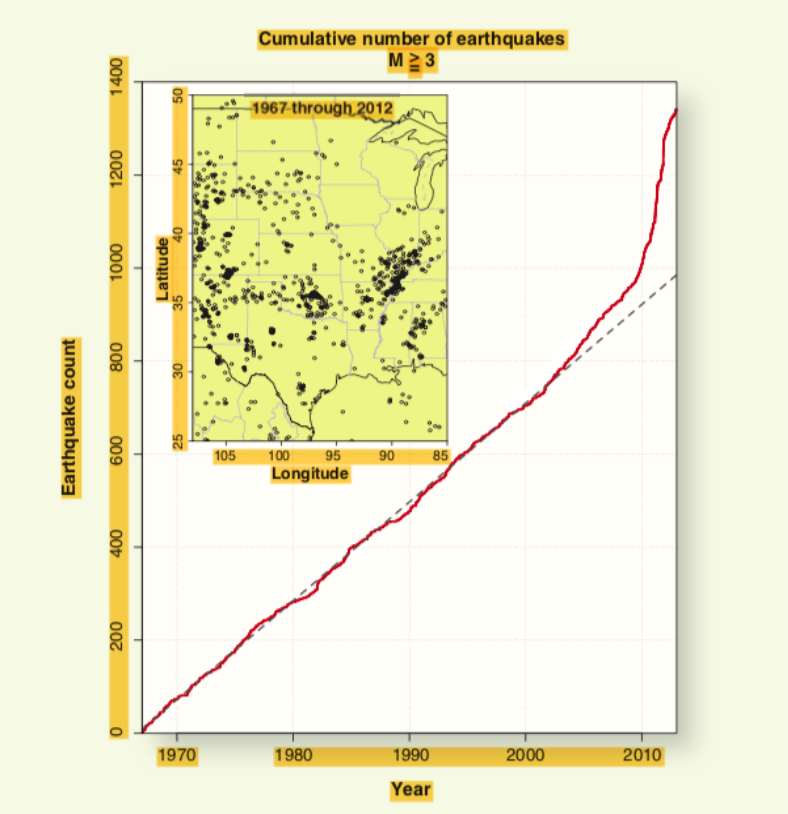

Fig 2: Cumulative count of earthquakes with M ≥ 3 in the Central and Eastern United States between 1967 – 2012 [Ellsworth, 2013].

Gouge Layer

Many experimental investigations operate on the assumption of faults not considering fault gouge. However, in natural rock, active faults will have a layer of gouge between the fault blocks, being another reason why slip under conditions of fluid pressurization are poorly constrained [French *et al.,* 2016]. Gouge layer has an effect on shear stress required to accommodate movement. Low stress rock friction is dependent on surface roughness. At high normal stress, friction is almost independent of the rock type. A gouge layer can reduce the friction to very low levels [Byerlee, 1978]. The magnitude of velocity

strengthening varies inversely with normal stress and directly with gouge thickness and fault surface roughness. The slip rate of the fault also is directly related to gouge thickness and surface roughness. This would explain why accumulation of gouge may stabilize slip and cause aseismic slip [Marone *et al.,* 1990]. Permeability of the gouge layer is also a contributing factor to fault slip. Grain size in the gouge is an important factor in determining permeability of the gouge layer. Coarse-grained gouges are observed to be the most permeable and fine-grained gouges are observed to have lower permeability [Morrow *et al.,* 1984]. Both fine- and coarse-grained gouges decrease in permeability after shearing [Morrow *et al.,* 1984]. A low permeability can lead to lower shear stress. The shear localization also varies with gouge grain size, which changes exactly where the fault will slip.

V. HYPOTHESIS

Wastewater well injection is causing an increase in seismic activity. The presence of pore fluid will affect critical shear stress. In addition, recent experiments do not take into the account of a gouge layer along the fault. Different pore fluid pressures will have an effect on slip behavior when a gouge layer is included in the experiments. Increasing pore fluid pressure leads to lower critical stress threshold and subsequent fault slip. Results of this work will have a bearing om understanding wastewater well injection causing increases in seismic activity.

VI. METHOD OF ANALYSIS

Experimental Design

In order to test the effects of gouge on slip instability, I simulated slip between two blocks of Berea Sandstone with a quartz gouge layer between the two blocks, attempting to replicate a fault. Berea Sandstone was used because of its high porosity and permeability. Quartz was used in the gouge layer because it occurs frequently in natural rock. The rock sample was prepared, discussed later, and loaded into a programmable, controlled conventional triaxial deformation apparatus [Fig. 3 and Fig. 4] that can control the pressures acting on the sample, by servo control. The servo controlled hydraulically powered intensifiers, control the confining pressure, *Pc*, axial load, $\sigma 1$, and pore fluid pressure, *Pf*, by applying the pressure under servo feedback control. This servo control minimizes fluctuations in experimental conditions that significantly reduces error of data collection. The apparatus then uses force gauges to collect voltages that can be converted to the resulting pressures acting on the sample. The simulated slip experiment was performed at four different conditions as seen in Table 1 below:

Experiment	**Condition**	**Confining Pressure**	**Pore Fluid Pressure**
1	Dry	70 MPa	0 MPa
2	Wet	75 MPa	5 MPa
3	Wet	100 MPa	30MPa
4	Wet	130 MPa	60MPa

Table 1: Trials descriptions with conditions. The differential stress between the two pressures remained at 70 MPa to keep consistency.

Under these four sets of conditions, the frequency of stick-slip, stress drop along the fault, and yield stress for each of these conditions were all observed and recorded. The results were analyzed and used to better characterize the effect of pore fluid pressure in faults with gouge.

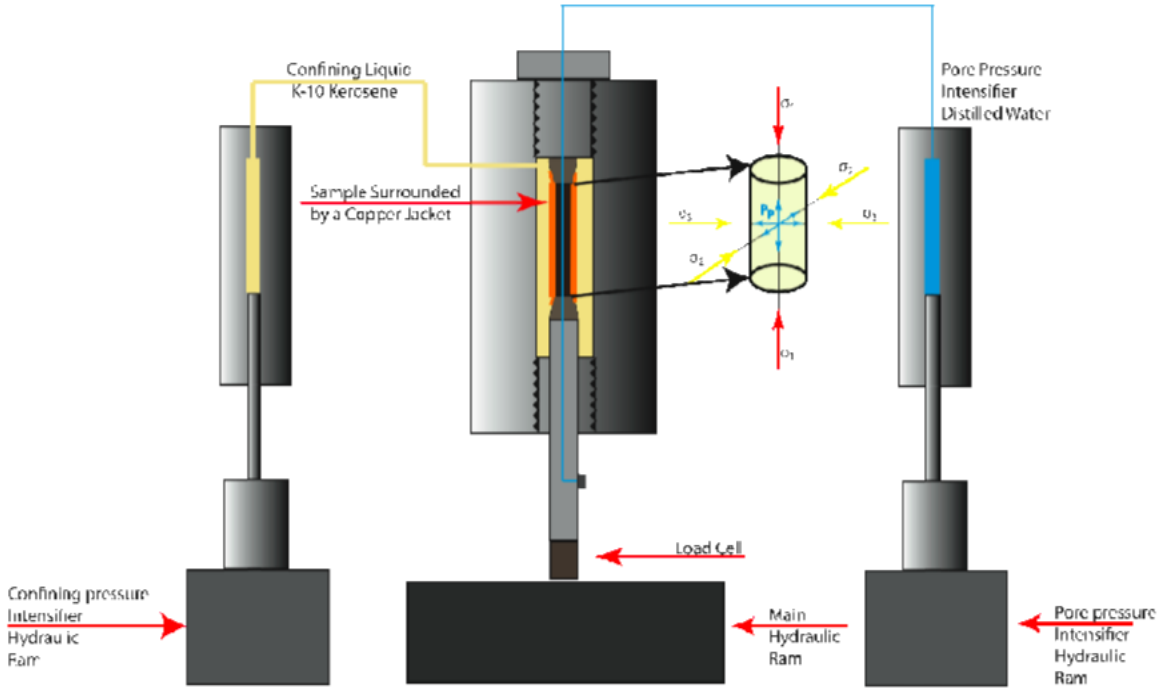

Fig 3: Diagram of triaxial deformation apparatus [Tamarkin, 2011].

Fig 4: Picture of triaxial deformation apparatus.

I investigated slip behavior on faults with gouge by simulating fluid pressurization on replicated gouge samples with varying different values of confining (Pc) and pore fluid pressures (Pf). The sample was loaded into a triaxial apparatus that continually increased its axial load (σ_1). The failure behavior of the sample was then be examined and compared. Before the sample was loaded into the apparatus it was first prepared and pre-compacted overnight. Pre-compaction includes setting the confinement pressure of the sample before the sample is loaded to ensure there is no leaks in the sample.

Fig 5: Berea Sandstone cylinder cut into two equal parts at 30° angle. Cylinder is put back together after gouge layer applied.

The Berea Sandstone sample started as a cylinder forcing block that is 25.4mm in diameter and 50.8 mm in length. The cylinder was then cut into two [Fig. 5] equal parts at a 30° angle from the base of the cylinder. This replicated faults in nature that are often oriented at a 30° angle. One half of the sample was then wrapped in a piece of copper that is was measured out with a previously cut template, prepared by the Laboratory for Rock Physics on the campus of University of Maryland College Park. The template allows for the copper wrap to properly hold a gouge layer on half of the cylinder. The copper wrap is soldered together tightly to keep it in place. The dry quartz sample was then weighed out to 0.5 grams and mixed with no more than 0.5 mL of water to create a paste. The grain size of the quartz sample used is less than 10 microns. Again, quartz is used because it is a common mineral in Earth's crust and the grain size was chosen to allow for large enough space in the gouge layer to allow for optimal results. The paste was then weighed and poured into the area of the sample created by the copper wrap. The paste was then set to dry by natural means [Fig. 6] or is accelerated with a heat gun. Once the gouge layer has mostly dried, the other half of the cylinder is put on top recreating the cylinder and sealing in the gouge layer [Fig. 7].

Fig 6: One half of the Berea Sandstone wrapped in the copper foil. The gouge layer was applied and allowed to dry before being sealed with the other half.

In order to properly gather results, the sample was sealed by a polyolefin heat-shrink sleeve mechanism that has the sample confined by ferro block rings, O-rings, and metal ties. This insures that while the apparatus in increasing the axial load on the sample, it will not leak or be affected by any outside parameters other than the ones being controlled. The sample sleeve [Fig. 8] will be loaded into the top of the apparatus and connected to the axial loading piston and fluid injection pipe. Before the experiment is run, the sample needs to be pre-compacted in the apparatus overnight with the desired confining pressure.

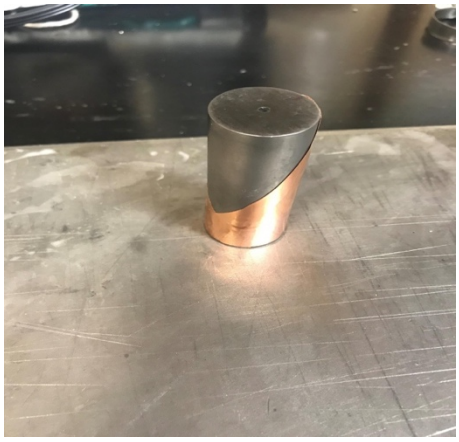

Fig 7: Picture of a sample in copper wrap and put back together. This is a picture of a stainless-steel forcing block instead of Berea Sandstone.

Experiment

This experiment was conducted at each of the four mentioned conditions. These data will be collected, and the resulting voltages will be converted into pressures and displacements using a MATLAB code designed for the apparatus, prepared by the Laboratory for Rock Physics on the campus of University of Maryland College Park. The MATLAB code using a variety of mathematical equations to appropriately convert the voltages to pressures and lengths. The code was prepared by graduate student, Tiange Xing. Using these data, I compared the frequency of slip on the samples, the stress drops across the samples, and the yield stress to characterize the effect the different pore pressures had on the slip behavior with a gouge layer involved.

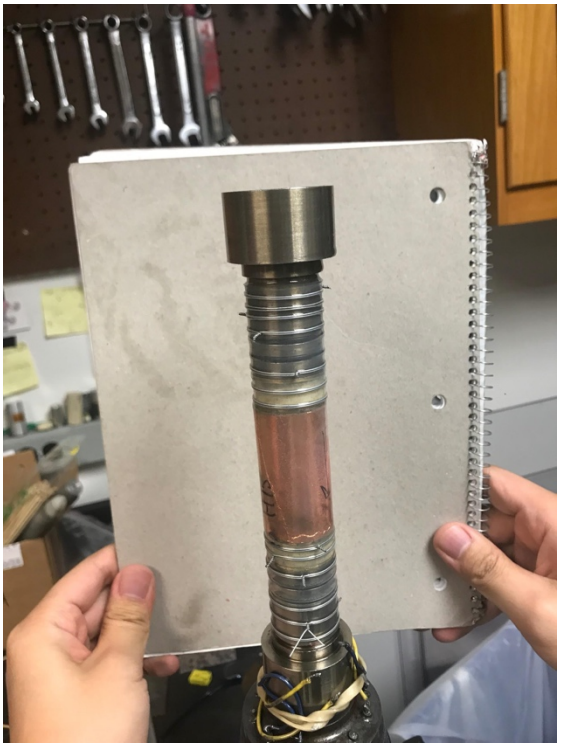

Fig 8: Picture of sample in loading jacket.

VII. PRESENTATION OF DATA, AND ANALYSIS OF UNCERTAINTY

Four experiments were conducted at the varying pressure conditions. The values for pressure conditions are graphed to show they were constant at the desired values throughout the experiments. The shear stress value on the sawcut versus the axial displacement of the loading ram is also graphed. These graphs show the slip behavior and desired observations of slip behavior; frequency of slip, stress drop, and yield stress. As the ram displacement of the triaxial apparatus increased, so did the differential stress on the sample. An expanded view of the graph

is provided to better see the behavior of the slip. These observations are done is for each experiment for comparison.

Experiment 1: Dry Condition P_c = 70 MPa and P_f = 0 MPa

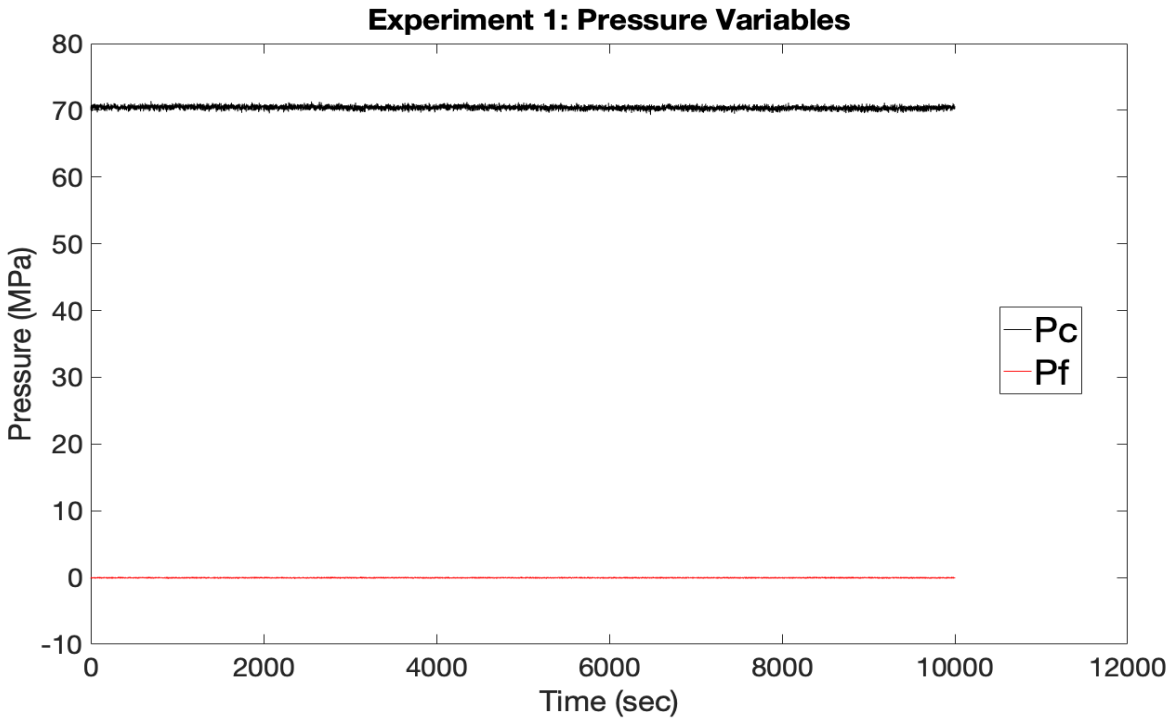

Fig 9: Pressure variables as measured by triaxial load apparatus. Pc = 70 MPa and Pf = 0 MPa. In order to properly set these values, the sample was pre-compacted, overnight in the triaxial apparatus at the desired confining pressure. This ensured there would be no leaking during the experiment. The fluid pore pressure injects distilled water into the sample. Both the pore fluid pressure and confining pressure are servo controlled. These data voltages were collected from the beginning to the end of the experiment and processed to show the values above.

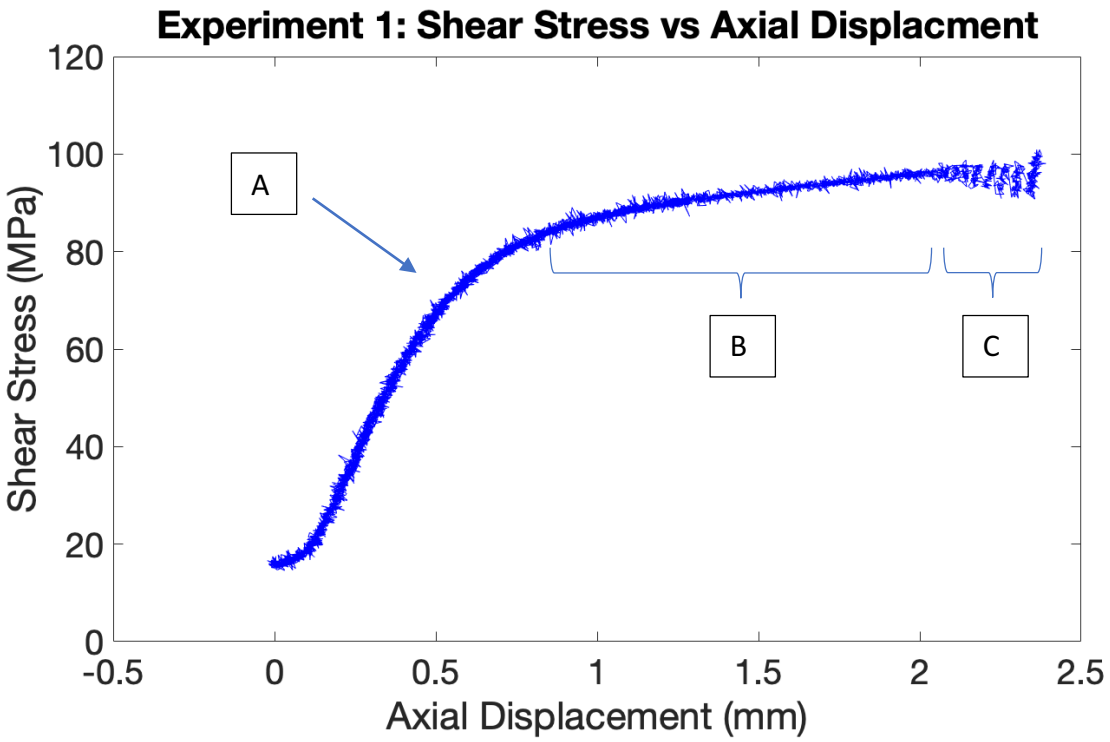

Fig 10: Shear stress as a function of axial displacement with Berea Sandstone forcing blocks and dry conditions (Pc = 70 MPa and Pf = 0 MPa). The shear stress data voltages are collected and processed and shown above. A.) At this point of the deformation, the graph starts to plateau. This means that the fault on sample has reached is yield stress and fails. This leads to seismic activity. B.) This area of the graph is aseismic behavior of the graph. This means the sample fault is failing but there is no slip. C.) This area of the graph shows the slip behavior of the sample. This is seismic behavior, as opposed to aseismic.

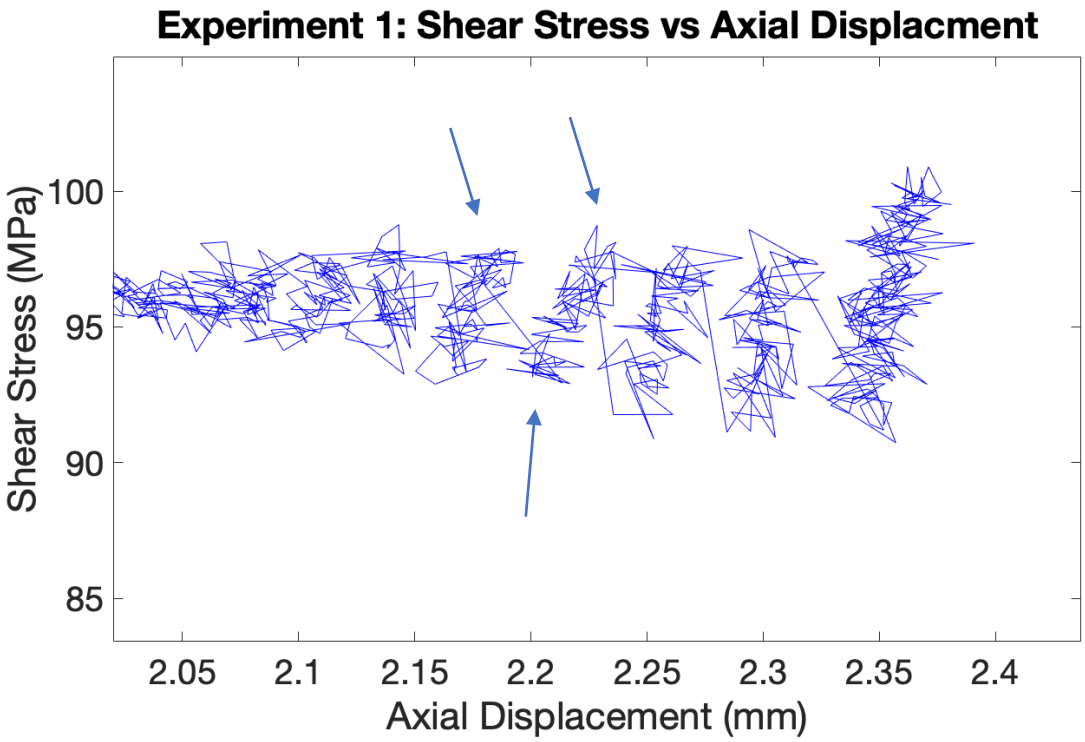

Fig 11: Close up of shear stress as a function of axial displacement with Berea Sandstone forcing blocks and dry conditions (Pc = 70 MPa and Pf = 0 MPa). Zoom is after first slip and focused on slip behavior. The arrows indicates example maximum and minimum values, or peaks, of the slip. The frequency and stress drops of this behavior were recorded and compared.

Experiment 2: Wet Condition P_c = 75 MPa and P_f = 5 MPa

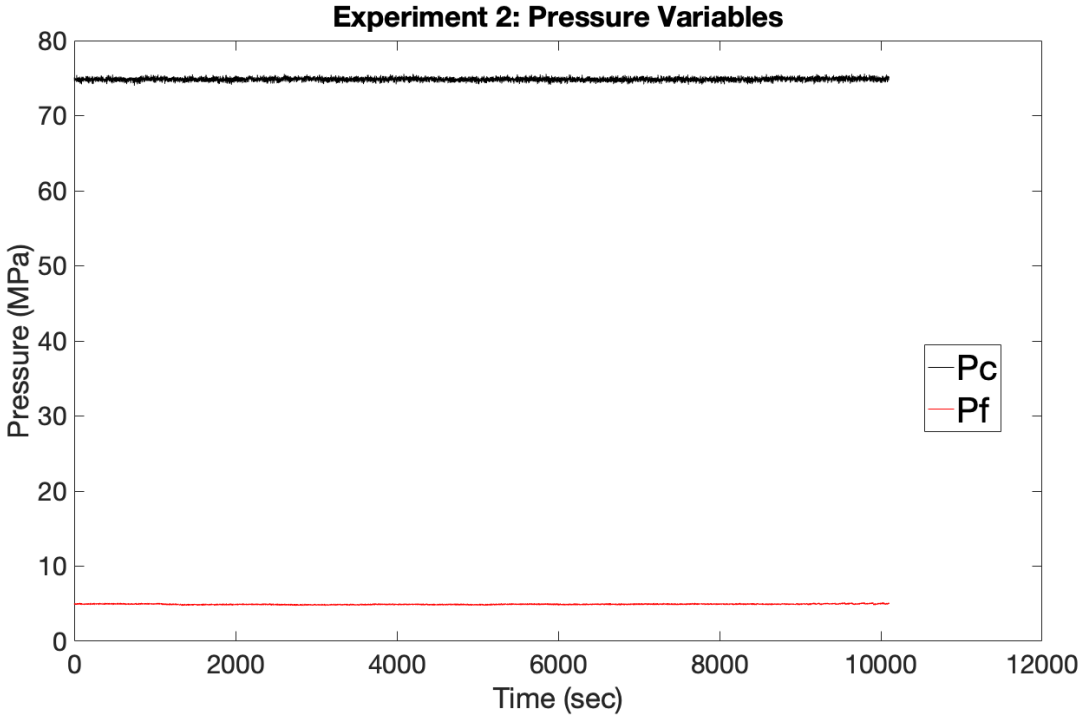

Fig 12: Pressure variables as measured by triaxial load apparatus. Pc = 75 MPa and Pf = 5 MPa. Identical to Experiment 1, the sample is pre-compacted, and the pressure variables are servo controlled. These data voltages are collected from the beginning to the end of the experiment and processed to show the values above.

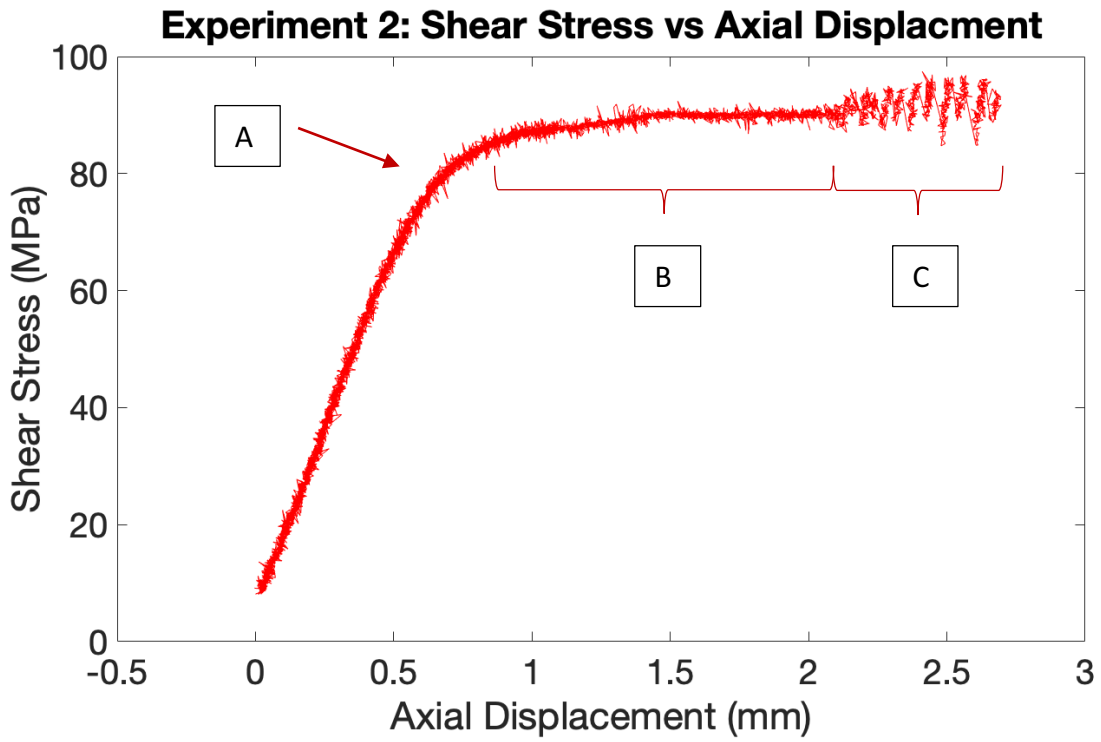

Fig 13: Shear stress as a function of axial displacement with Berea Sandstone forcing blocks and dry conditions (Pc = 75 MPa and Pf = 5 MPa). The shear stress data voltages are collected and processed and show above. A.) At this point of the deformation, the graph starts to plateau. This means that the fault on sample has reached is yield stress and fails. This leads to seismic activity. B.) This area of the graph is aseismic behavior of the graph. This means the sample fault is failing but there is no slip. C.) This area of the graph shows the slip behavior of the sample. This is seismic behavior, as opposed to aseismic.

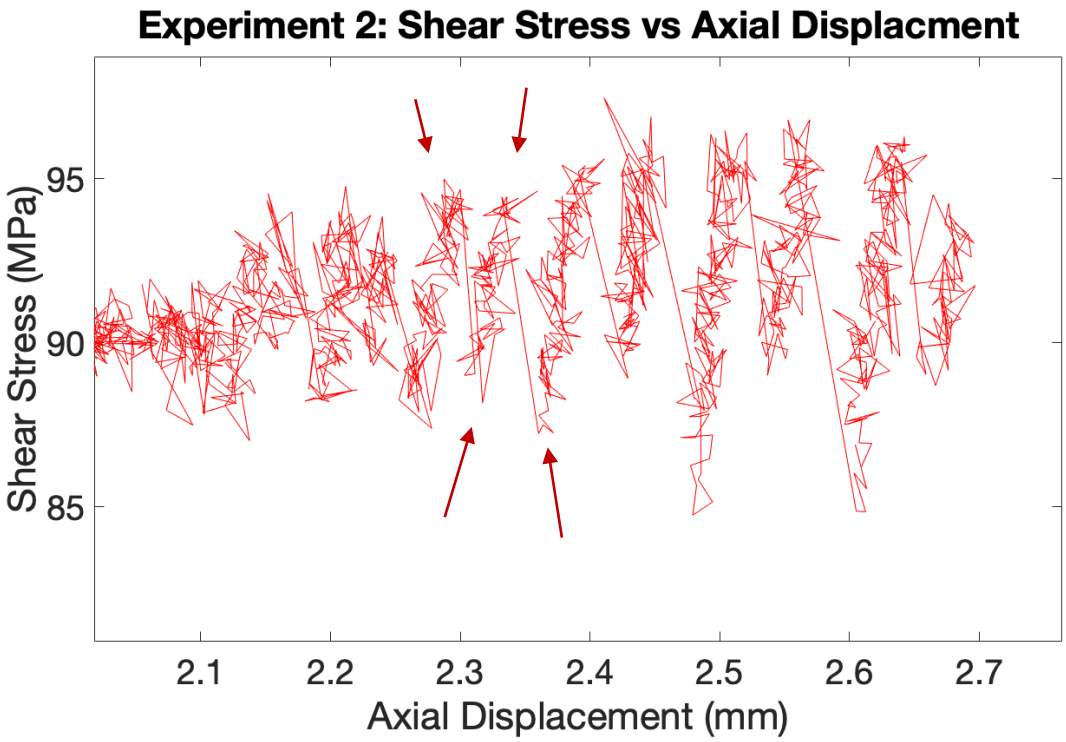

Fig 14: Close up of shear stress as a function of axial displacement with Berea Sandstone forcing blocks and dry conditions (Pc = 75 MPa and Pf = 5 MPa). Zoom is after first slip and focused on slip behavior. Zoom is after first slip and focused on slip behavior. The arrows indicate the maximum and minimum values, or peaks, of the slip. The frequency and stress drops of this behavior were recorded and compared.

Experiment 3: Wet Condition P_c = 100 MPa and P_f = 30 MPa

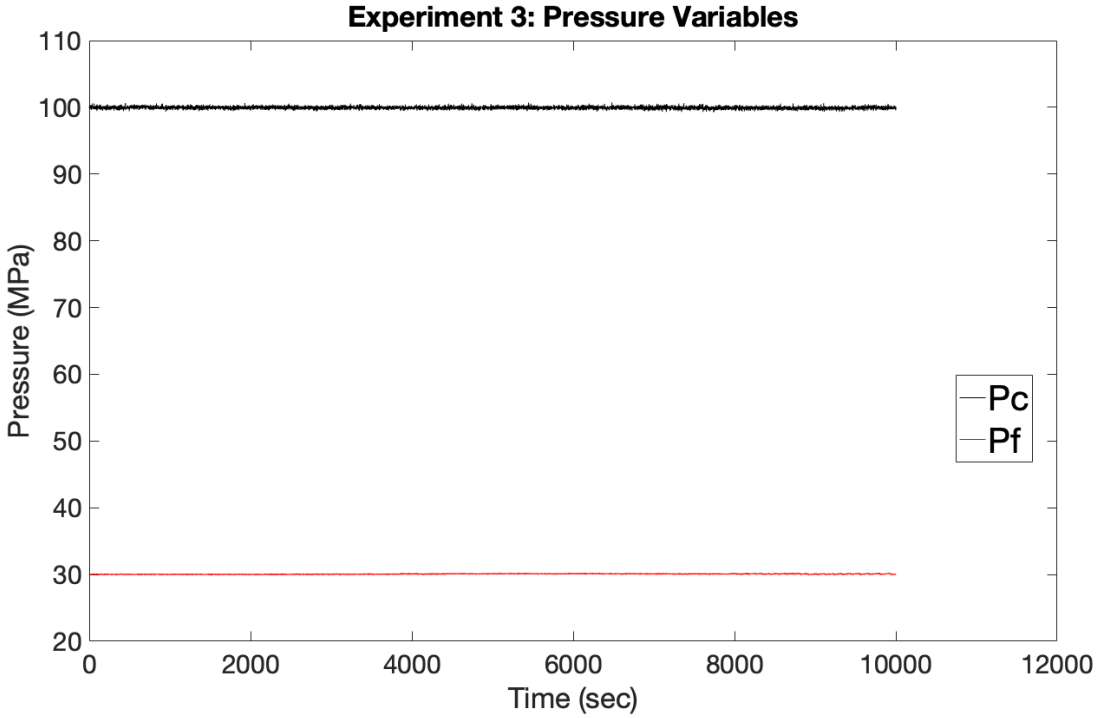

Fig 15: Pressure variables as measured by triaxial load apparatus. Pc = 100 MPa and Pf = 30 MPa. Identical to Experiment 1, the sample is pre-compacted, and the pressure variables are servo controlled. These data voltages are collected from the beginning to the end of the experiment and processed to show the values above.

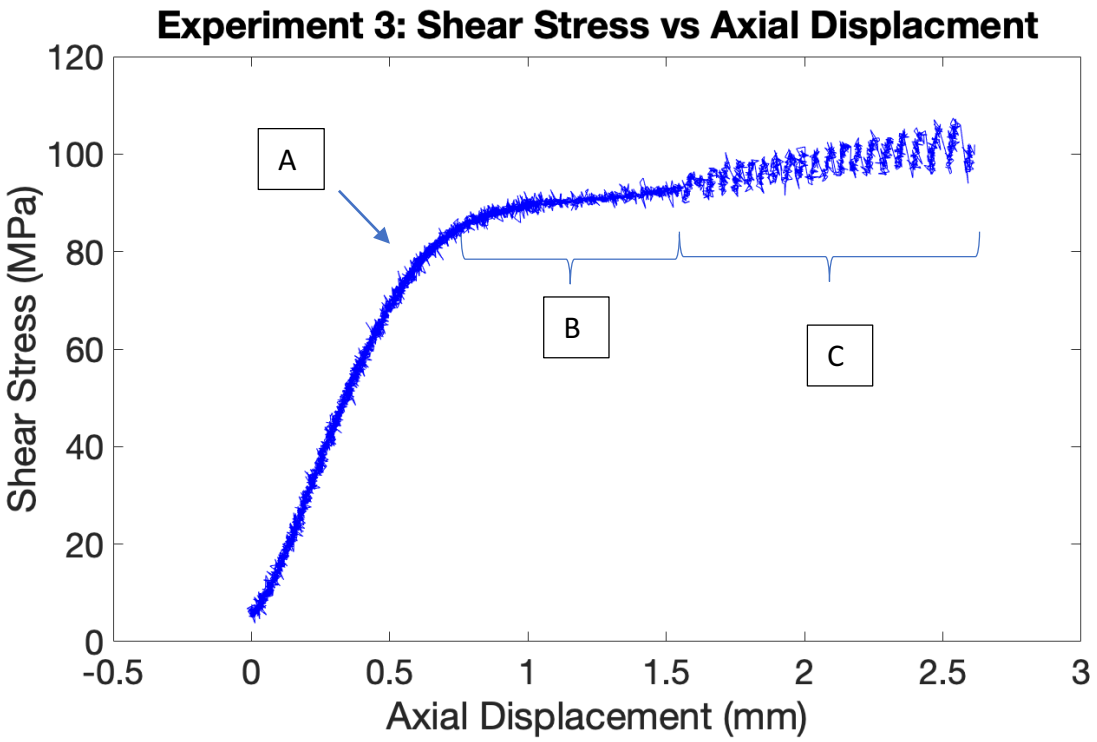

Fig 16: Shear stress as a function of axial displacement with Berea Sandstone forcing blocks and dry conditions (Pc = 100 MPa and Pf = 30 MPa). The shear stress data voltages are collected and processed and show above. A.) At this point of the deformation, the graph starts to plateau. This means that the fault on sample has reached is yield stress and fails. This leads to seismic activity. B.) This area of the graph is aseismic behavior of the graph. This means the sample fault is failing but there is no slip. C.) This area of the graph shows the slip behavior of the sample. This is seismic behavior, as opposed to aseismic.

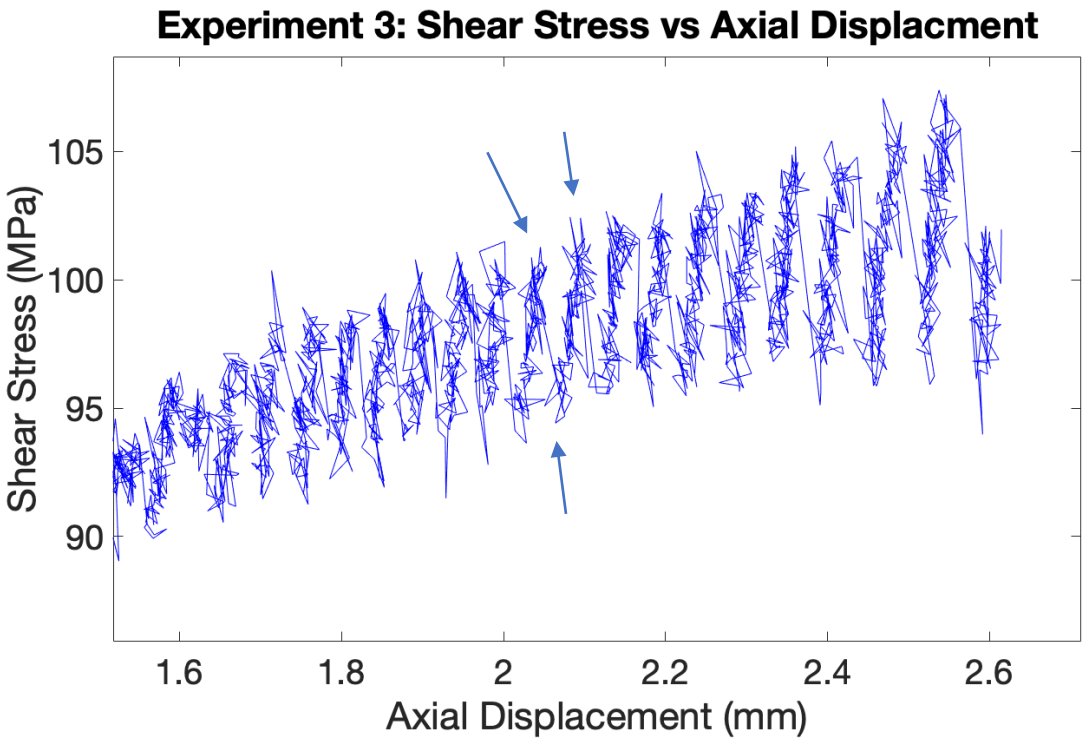

Fig 17: Close up of shear stress as a function of axial displacement with Berea Sandstone forcing blocks and dry conditions (Pc = 100 MPa and 30 = 5 MPa). Zoom is after first slip and focused on slip behavior. Zoom is after first slip and focused on slip behavior. The arrows indicate the maximum and minimum values, or peaks, of the slip. The frequency and stress drops of this behavior were recorded and compared.

Experiment 4: Wet Condition P_c = 130 MPa and P_f = 60 MPa

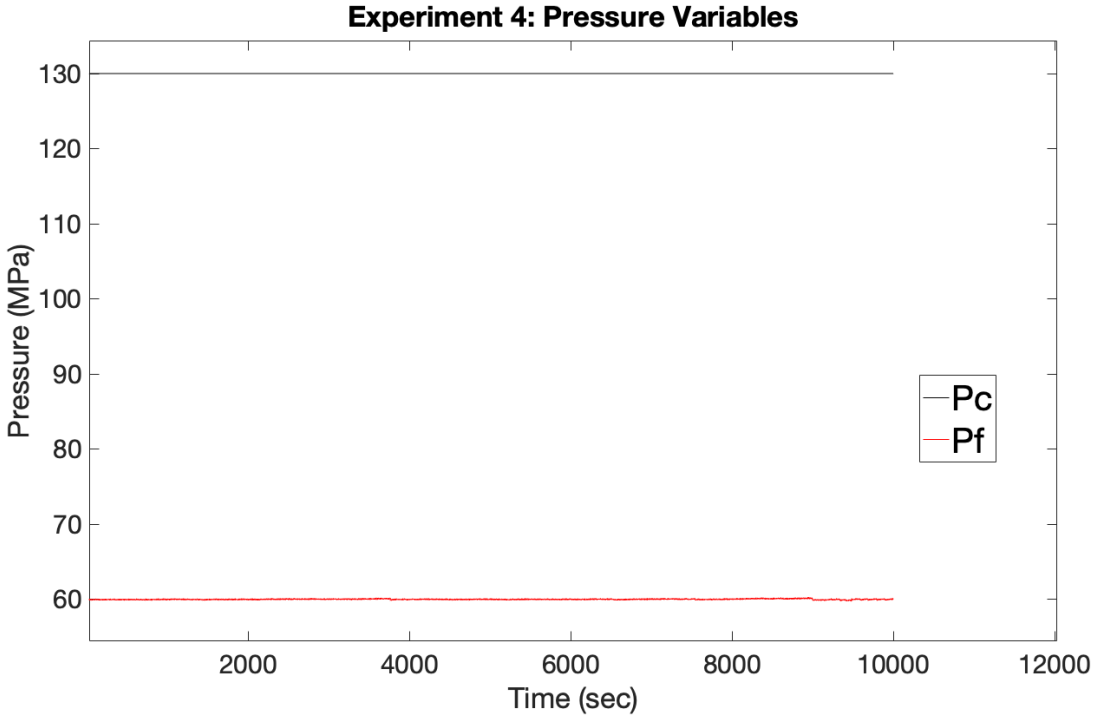

Fig 18: Pressure variables as measured by triaxial load apparatus. Pc = 130 MPa and Pf = 60 MPa. Identical to Experiment 1, the sample is pre-compacted, and the pressure variables are servo controlled. These data voltages are collected from the beginning to the end of the experiment and processed to show the values above.

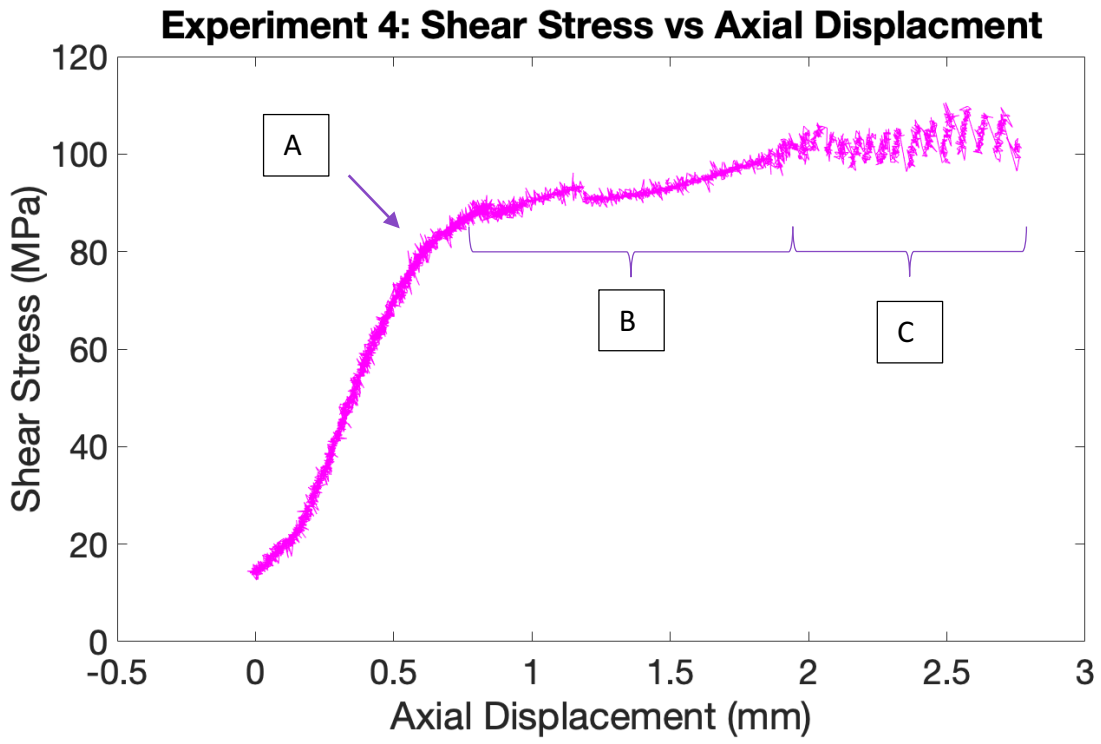

Fig 19: Shear stress as a function of axial displacement with Berea Sandstone forcing blocks and dry conditions (Pc = 130 MPa and Pf = 60 MPa). The shear stress data voltages are collected and processed and show above. A.) At this point of the deformation, the graph starts to plateau. This means that the fault on sample has reached is yield stress and fails. This leads to seismic activity. B.) This area of the graph is aseismic behavior of the graph. This means the sample fault is failing but there is no slip. C.) This area of the graph shows the slip behavior of the sample. This is seismic behavior, as opposed to aseismic.

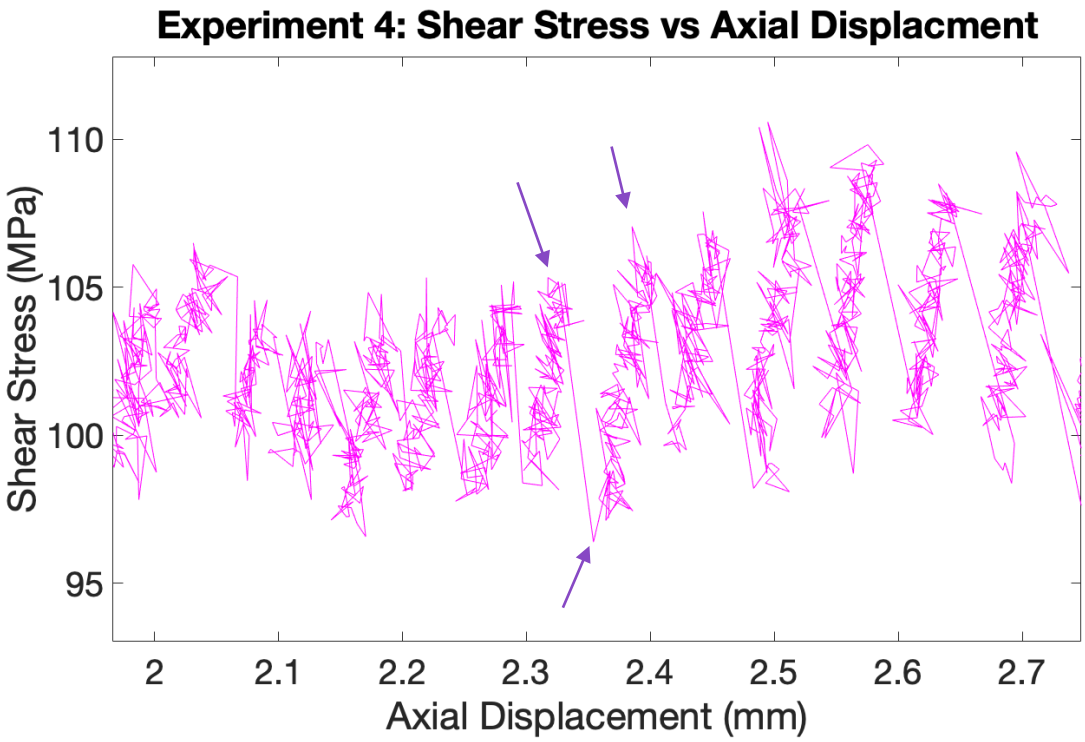

Fig 20: Close up of shear stress as a function of axial displacement with Berea Sandstone forcing blocks and dry conditions (Pc = 130 MPa and Pf = 60 MPa). Zoom is after first slip and focused on slip behavior. Zoom is after first slip and focused on slip behavior. The arrows indicate the maximum and minimum values, or peaks, of the slip. The frequency and stress drops of this behavior were recorded and compared.

Uncertainties

There are known uncertainties to take into account for this experimental investigation. Instrument resolution will only allow for certain precision to be made while measuring and weighing the samples. To make measurements a caliper with a resolution of 0.01 mm was used. To measure weight, a balance with a resolution of 0.00001 grams was used. The servo control in the triaxial apparatus minimizes fluctuations in experimental conditions which significantly reduces error of data collection. The range and precision of the triaxial load apparatus are seen in Table 2.

Sensor	Range and Precision
Confining pressure:	345 ± 0.9 MPa (50,000 ± 125 p.s.i.)
Main ram displacement:	154 ± 0.8 mm (6 ± 0.03 in)
Load cell-main ram:	3647 ± 4 MPa (529,000 ± 500 p.s.i.)
Pore fluid pressure:	137.9 ± 0.08 MPa (20,000 ± 11 p.s.i)
Pore volumometer:	61.86 ± 0.31 cm^3 (3.775 ± 0.019 in^3)
Strain Gauge:	350 ± 1.05 ohm

Table 2: Chart of range and precision of each sensor of the triaxial deformation apparatus.

The triaxial apparatus does produce noise that lead to uncertainty in data collection. There are uncertainties in data processing and MATLAB computation. To compensate for this, the MATLAB code that converts the voltages from the collected data takes into account factors that would cause uncertainties in data (temperature, area of slip) and makes correction for them. The corrections are never more than 0.1 MPa.

Sample Variation

Measurement uncertainty of the samples must also be taken into account due to heterogeneities in the sample leading to different values being obtained. The Berea Sandstone and quartz fault gouge are subject to some natural imperfections. There is some human uncertainty with preparing the samples as well.

VIII. DISCUSSION OF RESULTS

Experiment	Confining Pressure (MPa)	Pore Fluid Pressure (MPa)
1	70	0
2	75	5
3	100	30
4	130	60

Table 3: Table of pressure variables measured by in each experiment.

As explained by the above table, the pressures were appropriately servo controlled and allowed for the experiments to be ran at the desired conditions. This is important to the acceptability of my results and provides evidence that my variables were properly controlled. Although the machine's production of noise and other uncertainties were known and present, they did not limit the experiments due to the necessary precautions taken.

Experiment	Average Frequency of Slips (Hz)
1	0.013
2	0.012
3	0.011
4	0.010

Table 4: Table of average frequency of slips measured in each experiment. There is an inverse relation with pore pressure and frequency of slips, such that as the pore pressure increased, the frequency decreased.

The average frequency of the slip during failure decreased as the pore pressure increased. This means that seismic activity became less frequent as the pore fluid pressure increased. The decrease in frequency could be related to the stress drops being larger, shown in the table below.

Experiment	Average Stress Drop (MPa)
1	5.81
2	8.79
3	9.92
4	10.61

Table 5: Table of average stress drop during slip behavior measured by in each experiment. There was an increase in stress drop as the pore fluid pressure increased.

The average stress drops of the slip behavior increased as the pore pressure increased. The shear stress acting on the experimental fault has to rise to greater values to reach the critical shear stress and cause slip. This takes more time than a smaller stress drop, causing the decrease in frequency as mentioned above. The higher the stress drop, the more seismic the slip is. In real world application, this means a higher magnitude earthquake, ad a more hazardous seismic activity. Figure 21 shows the results of a sample after experiment 4. You can see the deformation and displacement of the two halves of the Berea Sandstone. In this experiment, increasing the pore fluid pressure from 0 to 60 MPa caused almost a 5 MPa difference in stress drop. Waste water wells use higher pressures than that of this experiment and can cause huge stress drops, leading to more hazardous seismic activity.

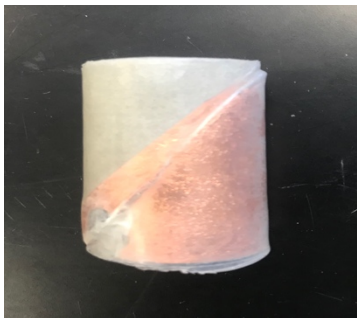

Fig 21: A sample after deformation and failure from experiment 4. The displacement of the fault can be seen. This replicates the displacement of a fault in nature.

Experiment	Approximate Yield Stress (MPa)
1	68.41
2	73.04
3	80.75
4	83.8

Table 6: Table of approximate yield stress observed in each experiment. As the pore fluid pressure increased, the yield stress of the sample increased.

As the pore fluid pressure increased, so did the yield stress of the sample. The yield stress is the value of shear stress where the sample fails and begins to begin seismic activity. A difference of 60 MPa caused the yield stress to increase by almost 20 MPa. The increase in pore fluid pressure in the sample caused the sample to reach higher levels of stress before failure. This is most likely due to the velocity strengthening from the gouge layer. The void space in the gouge layer allowed for the fluid in the sample, distilled water, to increase the strength of the rock and allow it to reach higher yield stresses. However, this can cause problems in real world applications. The operator of the wells may increase the pore fluid pressure to a value they think is safe, but the fault will still fail. Coupled with the increase in stress drops, this could lead to an unplanned hazardous seismic activity.

IX. SUGGESTIONS FOR FUTURE WORK

In future work, I would like to adjust a number of things from my experiment. First, I would like to have multiple trials of each condition. This would allow for more stable and efficient results to base my analysis off. I would also like to experiment with different grain sizes. The end goal of all these experiments would be to create an equation to determine critical shear stress from inputs such as gouge layer thickness, gain size, confining pressure, and pore fluid pressure.

X. CONCLUSIONS

With the increase in seismic activity due to wastewater fluid injection, characterization of fault slips will help avoid seismic hazards and save money and natural resources. However current characterizations of fault slip due to pressurization do not take into account a gouge layer along the faults, which is common in natural systems. By means of a triaxial apparatus, I investigated how the presence of different pore fluid pressures can affect the slip behavior of a fault with a gouge layer. I conducted four experiments of increasing pore fluid pressures; 0 MPa, 5 MPa, 30 MPa, and 60 MPa. While increasing the pore fluid pressure in a fault, I increased the normal stress on the sample until failure and observed the slip behavior. The increase in pore fluid pressure lead to a decrease in the frequency of slips during failure. The difference of 60 MPa in pore fluid pressure lead to a difference of 0.003 Hz. It also yielded a larger stress drop and higher yield stress. The stress drop increased from 5.81 MPa to 10.61 MPa, a difference of 4.8 MPa. A higher stress drop means greater seismic activity. The yield stress increased from

68.41 MPa to 83.8 MPa, a difference of 15.39 MPa. The higher yield stress means the sampled failed at greater shear stress value along the fault, meaning a a higher critical shear stress.

The presence of pore fluid pressure did affect the critical stress as hypothesized, however, it actually increased the stress value instead of lowering it like earlier predicted. The presence of a gouge layer strengthened the rock and lead to a higher yield stress required for failure. The different pore fluid pressures did have an effect on slip behavior as predicted. An increase in pore fluid pressure yielded a lower slip frequency, and higher stress drops.

With the increase in waste water wells, and subsequent seismic activity, this information is valuable to avoid seismic hazards. A geological explorer using wastewater wells will want to avoid injecting faults with high fluid pressure. Taking the gouge layer into account, the fault will have an increased critical shear stress, then one that is assumed without gouge. The explorer can increase the pore fluid pressure and assume the fault will not slip. However, the increase in pore fluid pressure will lead to higher stress drops and greater seismic activity. Higher magnitude earthquakes are a consequence of this and the waste water well could cause problems by causing these earthquakes. Most earthquakes caused by wastewater wells are below 3 in magnitude, but a high pore fluid pressure can raise the magnitude to a point where it affects the surface. If the use of waste water wells is to be continued, then geological scientist should understand how a gouge layer limits the amount of pore pressure they can subject a fault to, before it fails. They must also understand the consequences of the raised pore pressure, like a more seismic slip. Understanding the relation will help avoid future hazardous seismic activity from fluid injection.

XI. ACKNOWLEDGEMENTS

I would like to express my deep gratitude to Dr. Wenlu Zhu, my research advisors, for her patient guidance, enthusiastic encouragement, and availability as a resource. Her willingness to work with me every step of the way was very appreciated.

I would also like to extend my thanks to Tiange Xing for his assistance during my experiments and guidance and mentorship in and out the lab.

I would also like to extend my thanks to Dr. Takamasa Kanaya for his support and motivation.

Finally, I wish to thank James Bader, Goeun Ha, and Zachary Zega for their encouragement and feedback. It was very helpful and appreciated.

XII. Appendix

Experiment 2 Variation

During my investigation feasibility and reproducibility needed to be demonstrated. In doing this I repeated Experiment 2 a total of three times. These three trials were all run at the same pressure conditions. However, due to a combination of human error and less than adequate preparation, the sample was inefficient to collect data in the second trial. These data are displayed in three graphs below.

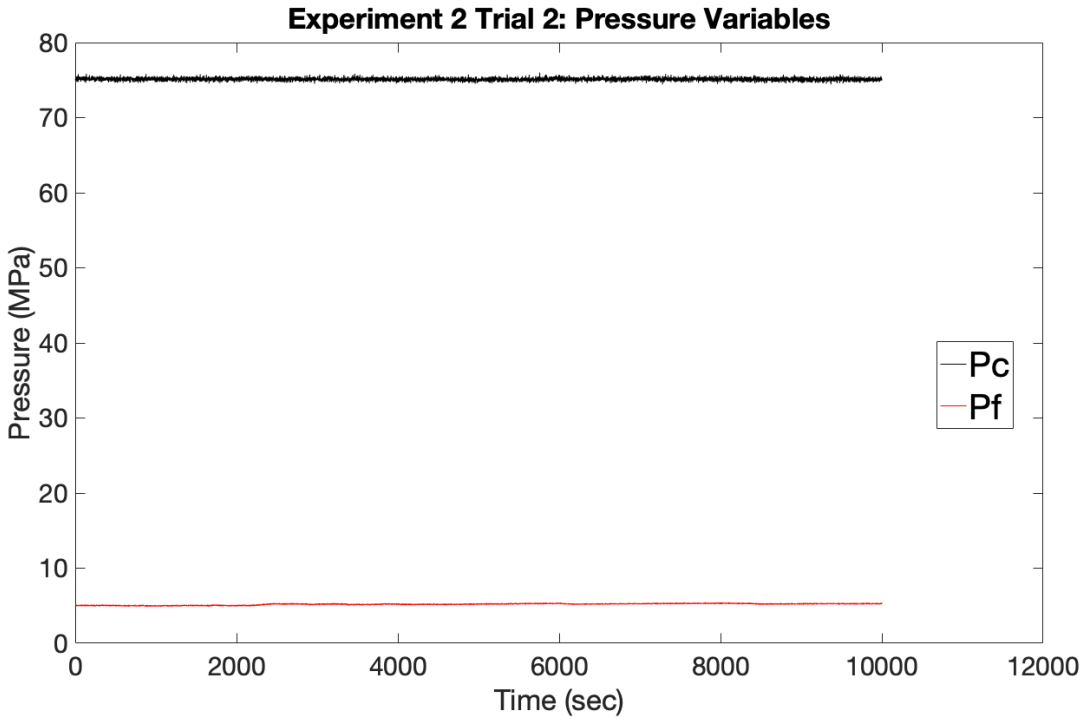

Fig 22: Pressure Variables as measured by triaxial load apparatus. Pc = 75 MPa and Pf = 5 MPa. These values were collected and used in the same method as previous discussed experiments.

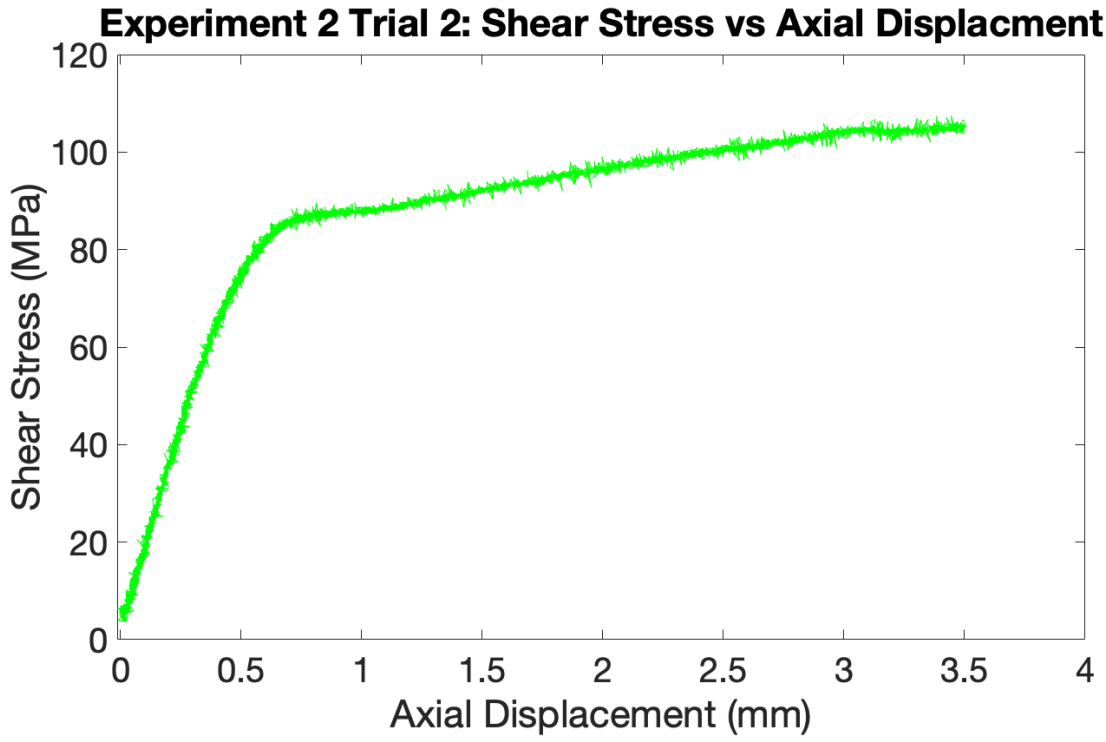

Fig 23: Shear stress as a function of axial displacement with Berea Sandstone forcing blocks and dry conditions (Pc = 75 MPa and Pf = 5 MPa). These values were collected and used in the same method as previous discussed experiments.

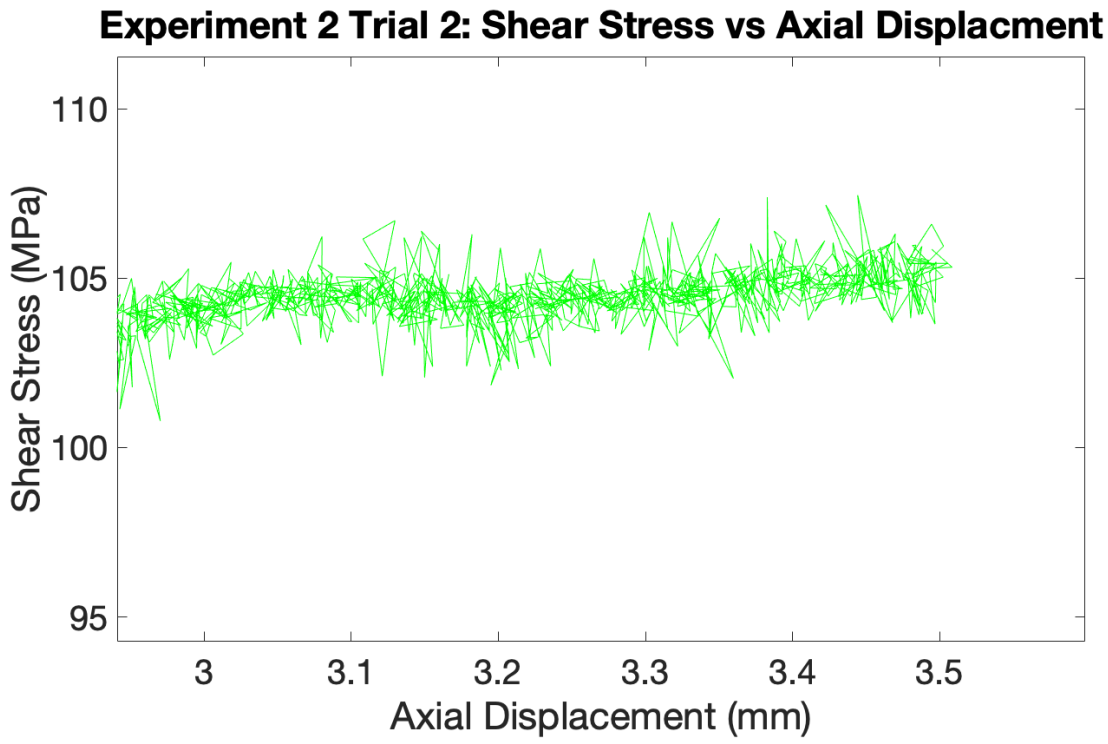

Fig 24: Zoom in of shear stress as a function of axial displacement with Berea Sandstone forcing blocks and dry conditions (Pc = 75 MPa and Pf = 5 MPa). Zoom is after first slip and focused on slip behavior. These values were collected and used in the same method as previous discussed experiments.

After collecting and processing these results, another experiment was conducted at the same conditions but refined the sample preparation process. This led to similar results as the first trial of these set of conditions. The results are shown below in three graphs.

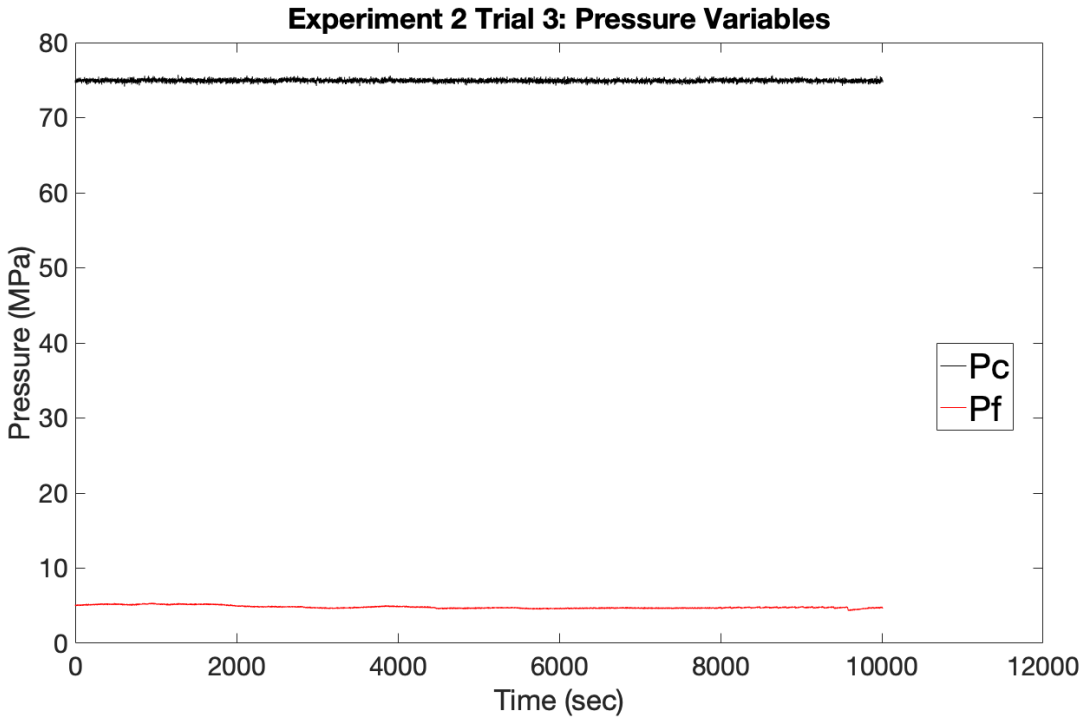

Fig 25: Pressure variables as measured by triaxial load apparatus. Pc = 75 MPa and Pf = 5 MPa. These values were collected and used in the same method as previous discussed experiments.

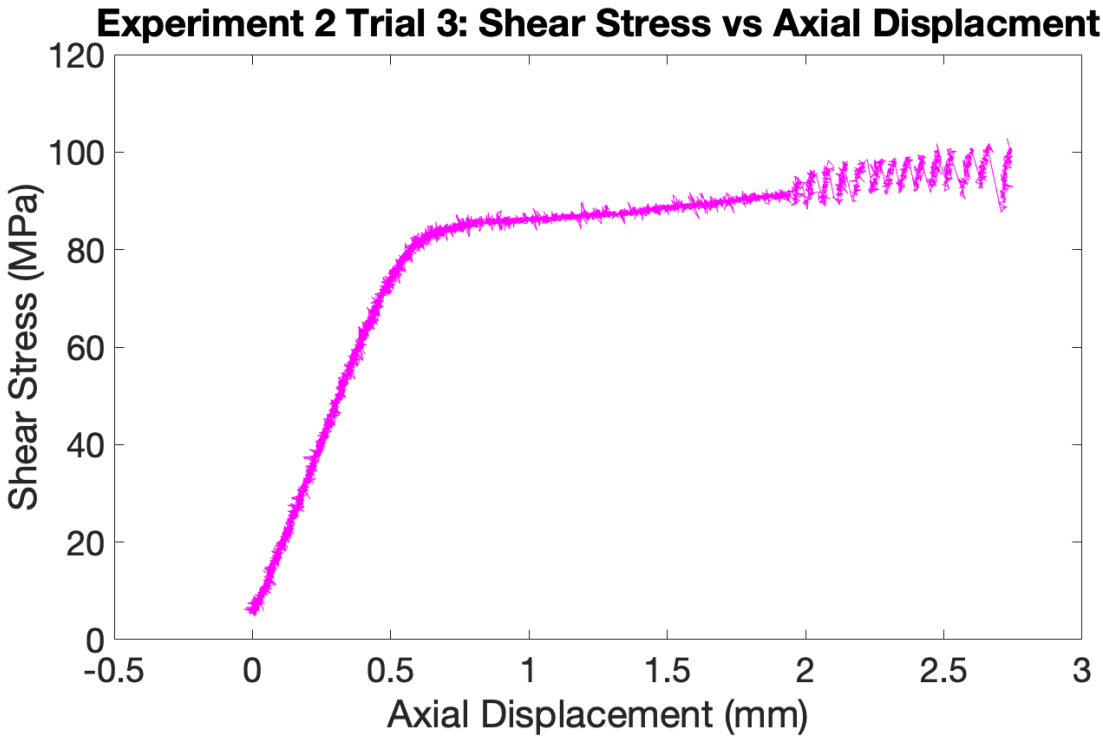

Fig 26: Shear stress as a function of axial displacement with Berea Sandstone forcing blocks and dry conditions (Pc = 75 MPa and Pf = 5 MPa). These values were collected and used in the same method as previous discussed experiments.

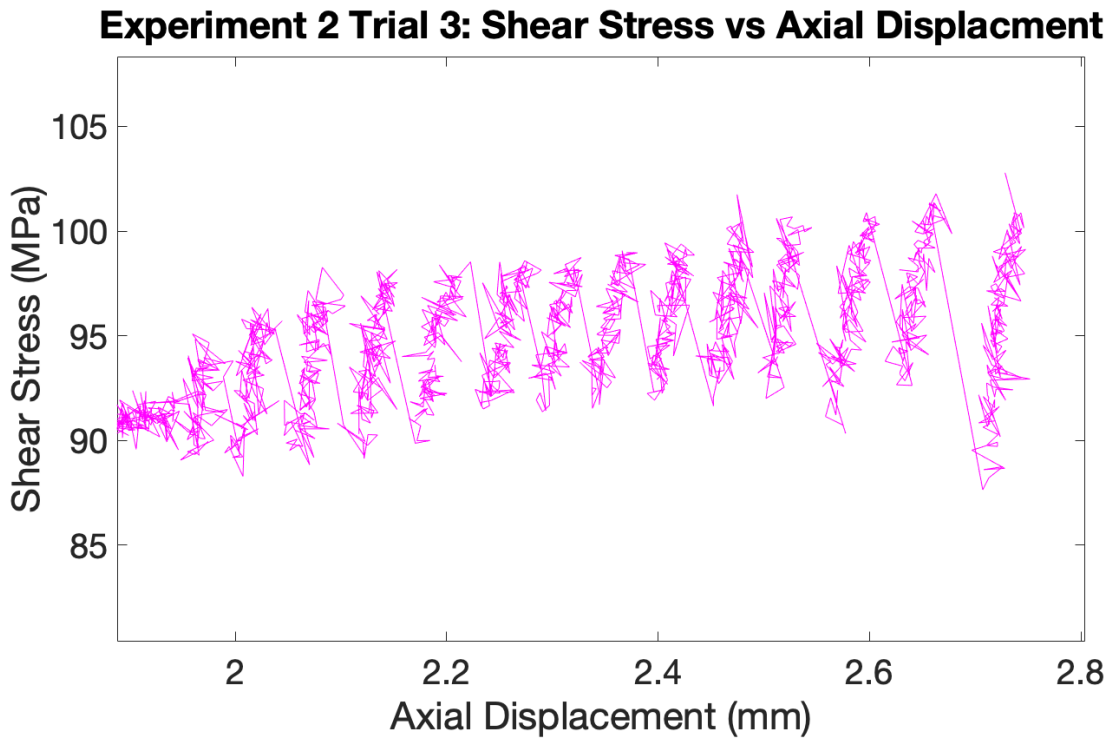

Fig 27: Close up of shear stress as a function of axial displacement with Berea Sandstone forcing blocks and dry conditions (Pc = 75 MPa and Pf = 5 MPa). Zoom is after first slip and focused on slip behavior. These values were collected and used in the same method as previous discussed experiments.

These results supported the idea that the results from the second trial were from human error and the results from the first trial were more accepted. The feasibility and reproducibility of the experiment was also supported. If more time was available, more trials of each experiment would have been conducted.

XIII. BIBLIOGRAPHY

Byerlee, J. "Friction of rocks." Rock friction and earthquake prediction. Birkhäuser, Basel, 1978. 615-626.

Ellsworth, W. L. "Injection-induced earthquakes." Science 341.6142 (2013): 1225942.

French, M. E., W. Zhu, and J. Banker. "Fault slip controlled by stress path and fluid pressurization rate." Geophysical Research Letters 43.9 (2016): 4330-4339.

Frohlich, C., J. I. Walter, and J. F. W Gale. "Analysis of transportable array (US Array) data shows earthquakes are scarce near injection wells in the Williston Basin, 2008–2011." Seismological Research Letters 86.2A (2015): 492-499.

Goebel, T. H. W., and E. E. Brodsky. "The spatial footprint of injection wells in a global compilation of induced earthquake sequences." Science 361.6405 (2018): 899-904.

Hillis, R. "Pore pressure/stress coupling and its implications for seismicity." Exploration Geophysics 31.1/2 (2000): 448-454.

Keranen, K. M., H. Savage, G. A. Abers, and E. S. Cochran. "Potentially induced earthquakes in Oklahoma, USA: Links between wastewater injection and the 2011 Mw 5.7 earthquake sequence." Geology 41.6 (2013): 699-702.

Keranen, K. M., M. Weingarten, G. A. Abers, B. A. Bekins, and S. Ge. "Sharp increase in central Oklahoma seismicity since 2008 induced by massive wastewater injection." Science 345.6195 (2014): 448-451.

Kim, W. "Induced seismicity associated with fluid injection into a deep well in Youngstown, Ohio." Journal of Geophysical Research: Solid Earth 118.7 (2013): 3506-3518.

Logan, J. M., and K. A. Rauenzahn. "Frictional dependence of gouge mixtures of quartz and montmorillonite on velocity, composition and fabric." Tectonophysics 144.1-3 (1987): 87-108.

Marone, C., C. B. Raleigh, and C. H. Scholz. "Frictional behavior and constitutive modeling of simulated fault gouge." Journal of Geophysical Research: Solid Earth 95. B5 (1990): 7007-7025.

Morrow, C. A., L. Q. Shi, and J. D. Byerlee. "Permeability of fault gouge under confining pressure and shear stress." Journal of Geophysical Research: Solid Earth 89. B5 (1984): 3193-3200.

Tamarkin, T. F. Progressive microscopic damage and the development of macroscopic fracture in porous sandstones. Master Thesis. 2011.

HONOR CODE

"I pledge on my honor that I have not given or received any unauthorized assistance on this assignment/examination."

Dashaun Horshaw
April 25, 2019